ELSEVIER

Journal of Alloys and Compounds 217 (1995) 128–136

Journal of ALLOYS AND COMPOUNDS

Phase equilibria in the systems Ti–C–N, Zr–C–N and Hf–C–N

S. Binder[a], W. Lengauer[a,*], P. Ettmayer[a], J. Bauer[b], J. Debuigne[b], M. Bohn[c]

[a]*Institute for Chemical Technology of Inorganic Materials, Vienna University of Technology, Getreidemarkt 9/161, A-1060 Vienna, Austria*

[b]*Laboratoire de Métallurgie et Physico-Chimie des Matériaux, CSIM, URA CNRS No. 1495, INSA Rennes, 20 Avenue des Buttes de Coësmes, F-35043 Rennes, France*

[c]*IFREMER, URA CNRS No. 1278, Centre de Brest, F-29280 Plouzané/Brest, France*

Received 2 June 1994

Abstract

The phase equilibria at 1150 °C in the solid regions of the systems Ti–C–N, Zr–C–N and Hf–C–N were investigated by means of arc-melted as well as hot-pressed alloys which were analysed for nitrogen and carbon and investigated by X-ray diffraction, metallography and electron probe microanalysis. In the Ti–C–N system the δ-Ti$(C_xN_{1-x})_{1-y}$ phase has a broader homogeneity range with respect to the ([C]+[N])/[Ti] ratio than do the f.c.c. boundary phases TiN_{1-y} and TiC_{1-y}. The subnitride phase ζ-Ti_4N_{3-x} does not perceptibly dissolve any carbon. In the Zr–C–N system the metal-rich phase boundary of the δ-Zr$(C_xN_{1-x})_{1-y}$ phase follows a nearly straight line between ZrC_{1-x} and ZrN_{1-x}. Phase diagrams of the Ti–C–N and Zr–C–N systems are presented. Owing to the low diffusion rates of carbon and nitrogen and the resulting inhomogeneous samples, the Hf–C–N system could be delineated but not clarified with respect to the phase equilibria where the hafnium subnitride phases are involved. Similarly to the δ-Ti$(C_xN_{1-x})_{1-y}$ phase, the δ-Hf$(C_xN_{1-x})_{1-y}$ phase has a broader homogeneity range than HfC_{1-y} and HfN_{1-y} have.

Keywords: Phase equilibria; Arc melting; Hot-pressed alloys; Homogeneity range

1. Introduction

The carbonitrides of the IVb metals are interesting materials for a number of high technology applications, e.g. as wear-resistant materials in cutting operations. They are used as powders for starting materials to produce sintered hard materials or as layers for wear-resistant and decorative coatings. While quite a number of studies are known for the binary carbide and nitride systems of these metals, the experimental information on the phase equilibria in the ternary carbonitride systems is restricted mainly to the quasi-binary MeC–MeN systems where complete miscibilities were observed. An attempt was made in the present study to clarify the phase relationships in the Ti–C–N, Zr–C–N and Hf–C–N systems.

1.1. Boundary systems

The binary carbide systems [1,2] Ti–C, Zr–C and Hf–C are characterized by the presence of one intermediate phase of the B1-type structure, a so-called δ phase, if the long-range ordering which is reported to take place in some carbon-deficient compositions [3] is not taken into account. These f.c.c. phases have an extensive homogeneity range. A critical compilation of the literature on the group IVb metal–carbon systems is contained in Ref. [4].

The binary nitride systems feature isotypic δ phases too, with comparable homogeneity ranges. The group IVb nitride systems are characterized by a high solubility of nitrogen in the low temperature modifications (α phases) of the metals as opposed to a low solubility of carbon. In the Ti–N and Hf–N systems the formation of various subnitride phases is observed, while these phases are absent in the IVb carbide systems as well as in the Zr–N system. For a more complete description of the Ti–N and Hf–N systems see Refs. [5–8].

The quasi-binary systems TiC–TiN, ZrC–ZrN and HfC–HfN feature complete solid solubility [9,10]. The most interesting physical properties of these compounds are presented in a separate paper [11].

*Corresponding author.

SSDI 0925-8388(94)01314-8

1.2. Ternary systems

An early study of the TiC–TiN system was performed by Agte and Moers [9] for the melting points of Ti(C,N) solid solutions with a non-metal/metal ratio of unity. They observed a slight maximum at [TiC]/[TiN] = 1. Several authors measured the lattice parameters of $Ti(C_xN_{1-x})_{\approx 1.00}$ [10,12,13]. For the lattice parameter, addition behaviour [12,13], $a(Ti(C_xN_{1-x})_{1.00}) = xa(TiC) + (1-x)a(TiN)$, as well as slight deviations from this rule [10] have been observed. Grieveson [14] measured the lattice parameters within the entire phase field of $Ti(C_xN_{1-x})_{1-y}$ and Mitrofanov et al. [15] investigated the extent of its phase field at 1923 K, finding that the ([C] + [N])/[Ti] ratio of the δ phase in equilibrium with α is about 0.45 for [C]/([C] + [N]) = 0.50. A systematic study of the phase equilibria at the relatively low temperature of 500 °C was performed by Arbuzov et al. [16], who reported an ordered δ' carbide phase which extended into the ternary Ti–C–N system. At this temperature the ϵ-Ti_2N phase was observed to dissolve carbon up to [C]/([C] + [N]) = 0.30.

The thermodynamics of $Ti(C_xN_{1-x})_{\approx 1.00}$ in equilibrium with nitrogen gas has been investigated by several authors [14,17–19]. In particular, Kieffer et al. [19] studied the nitridation behaviour of TiC at pressures up to 30 MPa. Decreasing temperatures and increasing nitrogen pressures shift the equilibrium between $Ti(C_xN_{1-x})$, carbon and nitrogen towards nitrogen-rich carbonitride compositions. Similar results were reported by Pastor [20].

Grieveson [14] tried to measure nitrogen activities of $Ti(C_xN_{1-x})_{1-y}$ by equilibrating it with nitrogen at low pressure, which was established by passing Ar over Si–Si_3N_4 mixtures. The Ti-rich corner of the ternary Ti–C–N system was investigated by Stone and Margolin [21] at four different temperatures up to 1300 °C. An increase in carbon solubility upon introduction of nitrogen into the α lattice was observed.

Thermodynamic modelling of the Ti–C–N system was performed by Teyssandier et al. [22] and Jonsson [23]. In the latter study ternary interactions in the various phases, except the β phase, were taken into consideration. The nitridation behaviour of TiC as described by Kieffer et al. [19] could be modelled well in Jonsson's work [23].

The lattice parameters in the ZrN–ZrC quasi-binary system were found to obey Vegard's rule [10,24,25]. The same investigations as in the TiC–TiN system were performed by Kieffer et al. [19] for the ZrC–ZrN system concerning the influence of nitrogen pressure and temperature on the composition of $Zr(C_xN_{1-x})_{1-y}$. It was found that the attainment of thermodynamic equilibrium is slower than for the TiC–TiN system and that the onset of reaction of ZrC with N_2 is at higher temperatures than of TiC with N_2.

Danisina et al. [26] investigated the Zr–C–N system at 1650 °C and proposed a phase diagram which, if the placement of samples with respect to composition is taken into consideration, is of quite speculative character.

Very few studies have been performed for the investigation of phase equilibria in the Hf–C–N system. Similar to studies in the Ti–C–N and Zr–C–N systems, Kieffer et al. [19] also investigated the reaction of HfC with nitrogen. The reaction rate was found to be very slow, probably reflecting the very low diffusivity of N and C. The lattice parameter in the HfC–HfN quasi-binary system changes linearly with the [HfC]/[HfN] ratio [10,27–29].

For Ti–C–N the only systematic study of solid–solid phase reactions was performed at $T = 500$ °C [16], which is quite low, since titanium carbonitrides are frequently used at $T > 1000$ °C. The phase reactions for the Zr–C–N system have been poorly investigated [26] and those for the Hf–C–N system not investigated at all. Therefore this project was undertaken to study the solid–solid phase equilibria in all three systems systematically.

2. Experimental details

Carbides, carbonitrides and nitrides in powdered form from H.C. Starck, Berlin were used as starting materials. The specifications for these powders are given in Ref. [11]. In addition, Ti powder as well as Zr and Hf sponges as listed in Table 1 were used. Zr and Hf sponges were hydrided in an H_2 atmosphere at 600 °C and powdered in a mortar.

For arc melting, the starting powders were mixed and cold pressed. Prior to arc melting, the hydride-containing samples were heated to 1000 °C in a vacuum in order to decompose the hydride, thereby avoiding rapid decomposition in the furnace which would cause ejection of the melt in the arc furnace. Arc melting was performed in a Ti-gettered Ar atmosphere. During the arc-melting process the samples lost substantial amounts of nitrogen. For the Hf–C–N system difficulties were encountered because of the high melting points of HfC and HfN. The samples either lost much of the nitrogen or were incompletely melted. Figure 1 shows these results for the Hf–C–N samples.

In order to prepare nitrogen-rich samples, hot pressing of powder mixtures was performed in graphite dies at temperatures up to 2400 °C and at a pressure of 55 MPa. The powder mixtures were prepared as described above, but no dehydridation cycle was carried out prior to hot pressing; instead, the temperature was slowly increased to 900 °C to allow the moderate escape of hydrogen.

Table 1
Impurity contents of Ti powder and Zr and Hf sponges as given by the supplier

	Ti	Zr	O	C	N	Fe	Al	Na	Cl
Ti	>99.7%	–	0.106%	0.006%	0.001%	0.005%	–	0.06%	0.081%
Zr	<25 ppm	–	57 ppm	54 ppm	15 ppm	678 ppm	30 ppm	–	–
Hf	<25 ppm	1.86%	640 ppm	<30 ppm	22 ppm	175 ppm	210 ppm	–	–

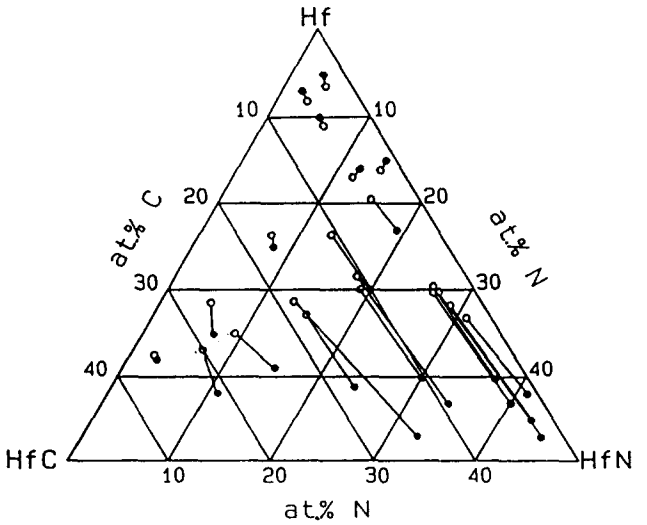

Fig. 1. Nitrogen loss during arc melting of HfC–HfN–Hf powder mixtures: ●, starting composition; ○, composition after arc melting.

Both the hot-pressed and the arc-melted samples were homogenized at 1300–1400 °C in an Mo crucible for 1–2 weeks, with the samples placed on coarse IVb carbonitride particles to avoid interaction with Mo. The carbonitrides were annealed on the same type of carbonitride bed.

Cut or coarsely crushed samples were placed in Mo foil and annealed in sealed silica tubes under an Ar atmosphere for 3 weeks at 1150±5 °C. After this equilibration treatment the capsules were quenched in water.

All samples which could be powdered were chemically analysed for carbon and nitrogen by Dumas gas chromatography (GC) [30]. The powdered samples were mixed with V_2O_5 as a combustion booster in a Sn crucible and oxidized in an He–O_2 atmosphere. The reaction products were analysed using a GC column. The accuracies are of the order of ±1 rel.% C or N respectively.

Standard metallographic and X-ray diffraction (XRD) characterizations of the samples were carried out (see e.g. Ref. [11]). Electron probe microanalysis (EPMA) was used in order to establish the tie-lines in multiphase samples for the Ti–C–N and Zr–C–N systems. A fully automatized Cameca Camebax SX50 microprobe with four spectrometers, two with crystals for light element analysis (W/Si multilayer crystals) and two with crystals for heavier elements (TAP and PET crystals), was used. Because of the coincidence of the N Kα and Ti L_1 lines, nitrogen could not be analysed directly but was taken as the balance for the Ti–C–N samples. Five $Ti(C_xN_{1-x})_{1-y}$ and four $Zr(C_xN_{1-x})_{1-y}$ homogenized and chemically characterized standards were used for calibration.

3. Results and discussion

3.1. The Ti–C–N system

Fig. 2 shows the phase diagram of the Ti–C–N system at 1150 °C which was established on the basis of 27 arc-melted and nine hot-pressed and equilibrated samples (Table 2). In addition, the Ti–C [4] and Ti–N [7] boundary systems are shown. It can be seen that the phase width of δ-$Ti(C_xN_{1-x})_{1-y}$ reaches lower values at medium [C]/([C]+[N]) ratios compared with the nitrogen or carbon contents in the binary nitride or carbide systems. This was established by microprobe analysis and with single-phase samples. The corners of the three-phase equilibrium $\alpha+\beta+\delta$ were determined by microprobe analysis on the basis of two independent samples; the obtained concentrations agreed well for the two sets of compositions (samples Ti L9 and Ti H9, arc melted and hot pressed respectively). These and further microprobe results for the tie-lines are contained in Table 3. The solid solution of N and C in α-Ti exists only at high nitrogen/carbon ratios. Because the lattice parameters of the subnitride phase ζ-Ti_4N_{3-x} did not change in different alloys, it is assumed that no nitrogen atoms can be replaced by carbon in this phase. This is in contrast with the results for the ϵ-Ti_2N phase, which was reported by Arbuzov et al. [16] to dissolve carbon up to [C]/([C]+[N])=0.30 at 500 °C.

The portion of the Ti–C–N system where phase equilibria with ζ-Ti_4N_{3-x} are involved could only be drawn tentatively, because no samples within the $\alpha+\zeta$ and $\zeta+\delta$ phase fields were obtained. This is due to the line compound character of ζ-Ti_4N_{3-x} [7] together with small inhomogeneities involved in the applied technique (see below).

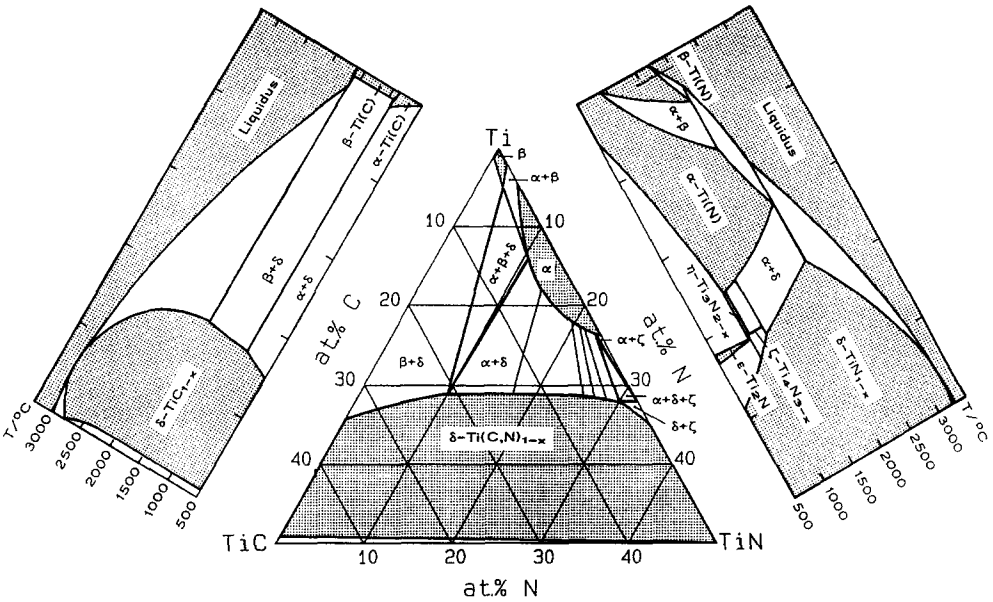

Fig. 2. Tentative phase diagram of the Ti–C–N system at 1150 °C together with boundary systems [4,7]. Four conodes are drawn in the $\alpha+\delta$ phase field.

Table 2
Results of gross chemical and metallographic analyses of Ti–C–N samples. Samples with * were ductile, could not be powdered and were therefore not analysed by Dumas GC. Because of negligible loss of nitrogen (and carbon) in samples of low metalloid content, the starting compositions were taken as the true sample compositions

Sample	C (wt. %)	N (wt. %)	C (at. %)	N (at. %)	Ti (at. %)	XRD results	Metallography results
Ti L1	3.45±0.01	7.74±0.05	10.7	20.5	68.8	δ, α	δ, α
Ti L2	6.62±0.22	5.13±0.15	20.0	13.2	66.8	δ	δ, (β)
Ti L3	10.65±0.15	2.66±0.04	30.7	6.6	62.7	δ	δ, (β)
Ti L4	4.45±0.01	6.30±0.01	13.8	16.8	69.4	δ, α	δ, α, (β)
Ti L5	9.54±0.18	2.68±0.06	28.2	6.8	65.0	δ, (α)	δ, (β)
Ti L6	2.27±0.16	7.65±0.04	7.2	20.7	72.1	δ, α	δ, α
Ti L7	5.77±0.06	3.55±0.04	18.3	9.6	72.1	δ, α	δ, β, (α)
Ti L8	2.25±0.02	4.74±0.02	7.6	13.7	78.7	δ, α	δ, α
Ti L9	4.64±0.04	3.21±0.06	15.2	9.0	75.8	δ, α	δ, α, β
Ti L10	2.09±0.03	3.29±0.05	7.3	9.9	82.8	δ, α	δ, α, β
Ti L11	0.98±0.03	3.57±0.03	3.5	10.9	85.6	α, (δ)	α, β, (δ)
Ti L12	*	*	2	3	95	α	α, β
Ti L13	1.14±0.03	10.77±0.04	3.5	28.5	68.0	δ, (ε)	δ, α, (ε)
Ti L14	0.64±0.03	9.84±0.07	2.0	26.8	71.2	α, δ, ζ, ε	α, δ, ζ, ε
Ti L15	1.61±0.03	9.42±0.03	5.1	25.2	69.7	δ, α	δ, α
Ti L16	0.65±0.03	9.33±0.04	2.1	25.6	72.3	α, δ, ζ, (ε)	α, δ, ζ, (ε)
Ti L17	1.22±0.02	9.00±0.04	3.9	24.6	71.5	α, δ	α, δ
Ti L18	5.02±0.02	7.21±0.03	14.4	18.7	66.9	δ	δ
Ti L19	8.98±0.11	3.60±0.05	26.4	9.1	64.5	δ	δ, (β)
Ti L20	12.85±0.10	0.92±0.06	36.4	2.3	61.3	δ	δ, (β)
Ti L21	7.47±0.19	1.81±0.03	23.5	4.9	71.6	δ, α	δ, β
Ti L22	0.77±0.09	2.65±0.06	2.8	8.3	88.9	α	α, β
Ti L23	*	*	9	1	90	δ, α	δ, β
Ti L24	0.49±0.06	6.19±0.03	1.7	18.1	80.2	α	α
Ti L25	*	*	5	3	92	δ, α	δ, β
Ti L26	*	*	4	1	95	δ, α	δ, β
Ti L27	*	*	1	1	98	α, (δ)	β, (δ)
Ti H1	*	*	1	33	66	δ	δ
Ti H2	*	*	2	31	67	δ	δ
Ti H3	*	*	7	26	67	δ	δ
Ti H4	*	*	1	24	75	α, δ, (ε)	α, δ, (ε)
Ti H5	*	*	16	16	68	δ	δ
Ti H6	*	*	19	12	69	δ	δ
Ti H7	*	*	36	0	64	δ	δ
Ti H8	*	*	3	9	88	α	α
Ti H9	*	*	7	5	88	δ, α	δ, α, β

Table 3
Microprobe results for phases in samples of the Ti–C–N system. Phases with * could not be analysed owing to the restricted lateral resolution of EPMA

Sample	Element	δ (at. %)	α (at. %)	β (at. %)
Ti L9	C	22.5	4.4	1.2
	Ti	68.1	87.6	95.5
	N	9.4	8.0	3.3
Ti H9	C	22.1	3.6	1.1
	Ti	67.3	85.6	95.4
	N	10.6	10.8	3.5
Ti L7	C	19.4		1.0
	Ti	70.0	*	94.1
	N	10.6		4.9
Ti L10	C		4.0	
	Ti	*	85.8	*
	N		10.1	
Ti L21	C	29.0		
	Ti	67.3	–	*
	N	3.7		
Ti L25	C	22.0		
	Ti	65.0	–	*
	N	12.0		
Ti L6	C	5.9	2.5	
	Ti	68.0	77.9	–
	N	26.1	19.6	
Ti H4	N	3.0	1.4	
	Ti	70.0	77.4	–
	N	27.0	21.2	
Ti L8	C	14.0	3.8	
	Ti	68.3	81.9	–
	N	17.7	14.3	
Ti L17	C	4.7	2.0	
	Ti	68.7	77.2	–
	N	26.6	20.8	
Ti L16	C		1.3	
	Ti	*	78.3	–
	N		20.4	
Ti L14	C	2.0		
	Ti	70.7	*	–
	N	27.3		

No literature values could be found for a direct comparison of these experimental results; the only available experimental studies are by Mitrofanov et al. [15] for $T=1650$ °C and the $Ti(C_xN_{1-x})_{1-y}$ phase only and by Arbuzov et al. [16] for 500 °C. The Arbuzov results could be excellently modelled by Jonsson [23].

The results of the thermochemical model for the Ti–C–N system by Jonsson [23] are in generally good agreement with those obtained here. In these calculations the ternary phase field $\alpha+\beta+\delta$ is narrower and the metal-rich phase boundary of $Ti(C_xN_{1-x})_{1-y}$ is nearly straight. The phase equilibria in the subnitride were not included in the calculations and hence cannot be compared with our experimental results.

3.2. The Zr–C–N system

Fig. 3 shows an isothermal section of the phase diagram of the Zr–C–N system. The microprobe data for these results as well as for establishing the two tie-lines are included in Table 4 and the gross compositions of the samples are listed in Table 5. Compared with the $Ti(C_xN_{1-x})_{1-y}$ phase, the metal-rich boundary of $Zr(C_xN_{1-x})_{1-y}$ runs as a nearly straight line between the metal-rich compositions in the boundary systems. The composition of the $Zr(C_xN_{1-x})_{1-y}$ phase in the equilibrium $\alpha+\beta+\delta$ shows a nitrogen-richer composition than the corresponding δ phase in the Ti–C–N system.

The tentative Zr–C–N phase diagram by Danisina et al. [26] at 1600 °C agrees qualitatively with our results for the metalloid-poor boundary of $Zr(C_xN_{1-x})_{1-y}$ despite the fact that they did not investigate the course of this boundary in detail. Completely different results were obtained by these authors for the compositions of the α-(Zr,C,N) phase and the δ phase in the $\alpha+\beta+\delta$ triangle. The α phase has a much lower metalloid content, thereby giving a different shape to the α phase field. The δ phase in this triangle is located at the Zr–C boundary side, thus the three-phase field is very narrow. The discrepancies cannot be explained by the different investigation temperatures and are probably due to the peculiar location of the samples; with these locations it is difficult for the reader to arrive unambiguously at roughly the same tentative phase diagram as the one presented by the authors [26].

Table 4
Microprobe results for several Zr–C–N samples

Sample	Element	δ (at. %)	α (at. %)
Zr L3	C	21.9	1.5
	N	14.9	12.4
	Zr	63.2	86.1
Zr L10	C	22.3	1.4
	N	14.8	12.2
	Zr	62.9	86.4
Zr L16	C	25.3	
	N	13.7	–
	Zr	61.0	
Zr L17	C	31.8	
	N	7.5	–
	Zr	0.7	
Zr L1	C	17.0	2.0
	N	21.3	15.8
	Zr	61.7	82.2
Zr L15	C	17.7	0.9
	N	18.9	13.4
	Zr	63.4	85.7

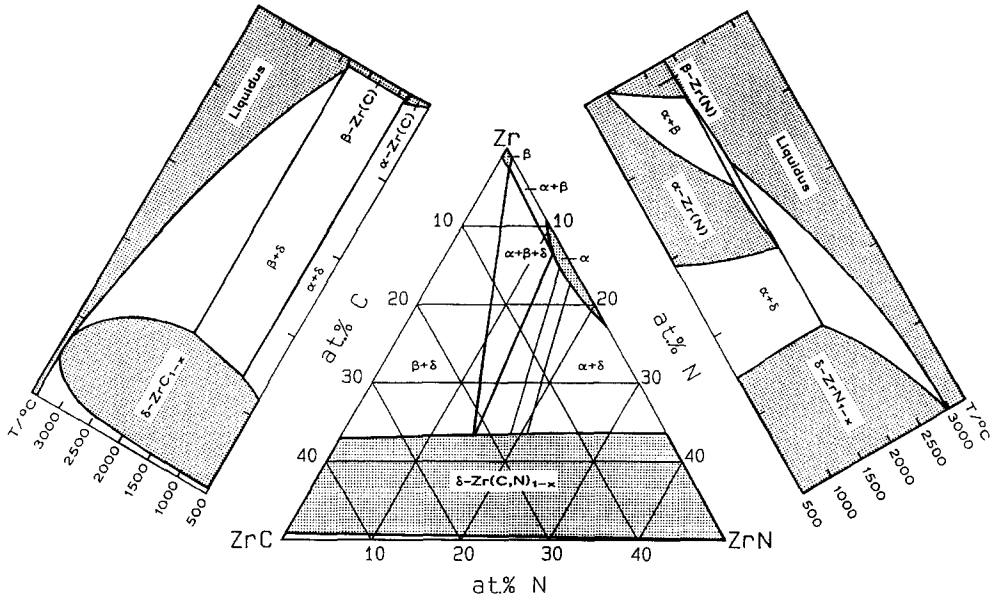

Fig. 3. Tentative phase diagram of the Zr–C–N system at 1150 °C together with boundary systems [4]. Two conodes are drawn in the $\alpha+\delta$ phase field.

Table 5
Results of gross chemical and metallographic analyses of Zr–C–N samples. Samples with * were ductile, could not be powdered and were therefore not analysed by Dumas GC. Because of negligible loss of nitrogen (and carbon) in samples of low metalloid content, the starting compositions were taken as the true sample compositions

Sample	C (wt. %)	N (wt. %)	C (at. %)	N (at. %)	Zr (at. %)	XRD results	Metallography results
Zr L1	1.12±0.03	3.43±0.2	6.7	17.7	75.6	δ, α	δ, α
Zr L2	4.34±0.04	1.96±0.03	23.6	9.2	67.2	δ, α	δ, β
Zr L3	2.32±0.03	2.32±0.01	13.8	11.8	74.4	δ, α	δ, β, α
Zr L4	1.05±0.07	2.94±0.08	6.4	15.6	78	δ, α	δ, α
Zr L5	4.52±0.11	1.28±0.06	25.1	6.1	68.8	δ, α	δ, β
Zr L6	*	*	13	8	79	δ, α	δ, β
Zr L7	0.92±0.02	2.23±0.03	5.9	12.3	81.8	δ, α	δ, α, (β)
Zr L8	*	*	15	2	83	δ, α	δ, β
Zr L9	*	*	10	5	85	δ, α	δ, β
Zr L10	*	*	5	7	88	δ, α	δ, α, β
Zr L11	*	*	4	2	94	δ, α	δ, α, β
Zr L12	*	*	1	4	95	α	α, β, (δ)
Zr L13	1.18±0.09	5.13±0.12	6.6	24.6	68.8	δ, α	δ, α
Zr L14	0.65±0.03	4.69±0.10	3.8	23.4	72.8	δ, α	δ, α
Zr L15	2.03±0.06	3.60±0.08	11.6	17.6	70.8	δ, α	δ, α
Zr L16	3.75±0.07	2.86±0.03	20.3	13.3	66.4	δ, α	δ, β
Zr L17	5.02±0.05	1.43±0.05	27	6.6	66.4	δ, α	δ, β
Zr L18	6.50±0.06	0.71±0.03	33.6	3.2	63.2	δ, (α)	δ, (β)
Zr L19	5.45±0.04	1.01±0.02	29.2	4.7	66.1	δ, α	δ, β
Zr L20	0.35±0.02	2.59±0.02	2.3	14.5	83.2	α, (δ)	α, (δ)
Zr L21	0.54±0.01	2.70±0.02	3.5	14.8	81.7	δ, α	δ, α
Zr L22	*	*	1	9	90	α, (δ)	α, β, (δ)
Zr L23	*	*	9	1	90	δ, α	δ, β
Zr L24	*	*	1	1	98	α, (δ)	α, β, (δ)
Zr H1	0.42±0.02	7.69±0.07	2.2	34.5	63.3	δ	δ, (α)
Zr H2	5.06±0.05	3.43±0.02	25.2	14.7	60.1	δ	δ
Zr H3	7.99±0.08	0.41±0.03	39.2	1.7	59.1	δ	δ
Zr H4	0.17±0.01	2.95±0.02	1.1	16.4	82.5	α	α

3.3. The Hf–C–N system

A total of 23 arc-melted and five hot-pressed samples were prepared for the phase equilibria investigations which are listed in Table 6. The Hf–C–N system is the only one in the series where the β phase does not occur at the investigation temperature.

No unambiguous proposal for the nitrogen-rich subnitride portion of the phase diagram could be derived from the results. Only the boundaries of the α and δ phase fields could be obtained from those samples in which the number of phases agreed with the phase rule. The scatter in the results for the subnitride region of the Hf–C–N system can be attributed to the unfavourable coincidence of low diffusion rates with the presence of line compounds. The arc-melted samples from powder mixtures contain more phases than allowed by the phase rule. This is of course not so obvious in samples without line compounds, so that the results obtained for the α and δ phase boundaries agree with the phase rule, although the gross homogeneity is certainly not better than that of the subnitride-containing samples.

A rough estimate can be obtained using the relationship $x=(D_\zeta t)^{1/2}$, where x is the mean diffusion distance and D_ζ is the diffusion coefficient of nitrogen in ζ-Hf_4N_{3-x}. D_ζ is 8.3×10^{-11} cm^2 s^{-1} as extrapolated from high temperatures to 1150 °C [31]. For a typical diffusion distance of 1 mm in arc-melted buttons an annealing time t of more than 33 000 h results. Therefore an increase in annealing time did not seem appropriate.

In addition to these difficulties, the formation characteristics of ζ-Hf_4N_{3-x} are not yet clear. It was observed that it does not form in annealing experiments with Hf metal in an N_2 atmosphere at temperatures lower than about 1200 °C [32]. However, once formed it does not decompose at temperatures lower than 1200 °C. The peculiar formation is influenced by the low diffusion rate of nitrogen. Recent investigations [33] showed that ζ-Hf_4N_{3-x} layer formation does not occur at this temperature if Hf metal is annealed in nitrogen. Instead, a Widmannstätten-type structure forms containing this phase.

The experimental results for the Hf–C–N system are presented in Fig. 4. Future investigations of the phase

Table 6
Results of gross chemical and metallographic analyses of Hf–C–N samples. Samples with * were ductile, could not be powdered and were therefore not analysed by Dumas GC. Because of negligible loss of nitrogen (and carbon) in samples of low metalloid content, the starting composition was taken as the true sample composition

Sample	C (wt. %)	N (wt. %)	C (at. %)	N (at. %)	Hf (at. %)	XRD results	Metallography results
Hf L1	0.32±0.02	2.87±0.20	3.4	26.5	70.1	α, δ, η, (ζ)	α, δ
Hf L2	0.31±0.01	3.17±0.01	3.2	28.5	68.3	α, δ, η, ζ	α, δ
Hf L3	0.38±0.02	2.83±0.01	4.0	26.1	69.9	α, δ, η, ζ	α, δ
Hf L4	0.23±0.05	3.49±0.01	2.3	30.8	66.9	α, η, ζ	α
Hf L5	0.35±0.03	2.77±0.02	3.8	25.7	70.5	α, δ, η	α, δ, η
Hf L6	0.96±0.01	1.89±0.02	10.6	17.7	71.7	α, δ	α, δ
Hf L7	1.02±0.01	2.02±0.01	11.0	18.6	70.4	α, δ	α, δ
Hf L8	1.73±0.02	1.70±0.03	17.9	15.0	67.1	α, δ	α, δ
Hf L9	2.59±0.04	1.05±0.01	26.0	9.0	65.0	α, δ	α, δ
Hf L10	2.52±0.03	0.55±0.01	26.5	4.9	68.6	α, δ	α, δ
Hf L11	3.64±0.01	0.32±0.01	35.1	2.6	62.3	δ, (α)	δ, (α)
Hf L12	0.40±0.04	1.41±0.11	4.8	14.7	80.5	α, δ	α, δ
Hf L13	0.91±0.02	1.10±0.06	5.2	11.8	83.0	α, δ	α, δ
Hf L14	0.37±0.02	0.50±0.04	4.9	5.8	89.3	α, δ	α, δ
Hf L15	0.38±0.01	0.25±0.01	5.2	2.9	91.9	α, δ	α, δ
Hf L16	1.73±0.03	1.44±0.02	18.2	13	68.8	α, δ	α, δ
Hf L17	3.08±0.06	0.81±0.04	30.1	6.8	63.1	α, δ	α, δ
Hf L18	0.90±0.02	1.03±0.02	10.5	13	76.5	α, δ	α, δ
Hf L19	1.42±0.01	0.72±0.03	16.5	7.1	76.4	α, δ	α, δ
Hf L20	0.16±0.01	1.29±0.04	2.0	14	84.0	α	α
Hf L21	0.19±0.03	0.32±0.03	2.6	3.8	93.6	α	α
Hf L22	*	*	5.0	0	95.0	α, (δ)	α, (δ)
Hf L23	*	*	2.0	0	98.0	α	α
Hf H1	2.25±0.02	2.56±0.02	20.8	20.2	59.0	δ, (α)	δ, (α)
Hf H2	1.41±0.01	3.28±0.01	13.3	26.4	60.3	α, δ	α, δ
Hf H3	0.64±0.01	4.81±0.03	5.8	37.1	57.1	δ, (ζ)	δ, (ζ)
Hf H4	0.28±0.01	4.07±0.04	2.7	34.2	63.1	η, (α)	η, α
Hf H5	0.30±0.01	4.62±0.01	2.9	37.1	60.0	δ, ζ	δ, ζ

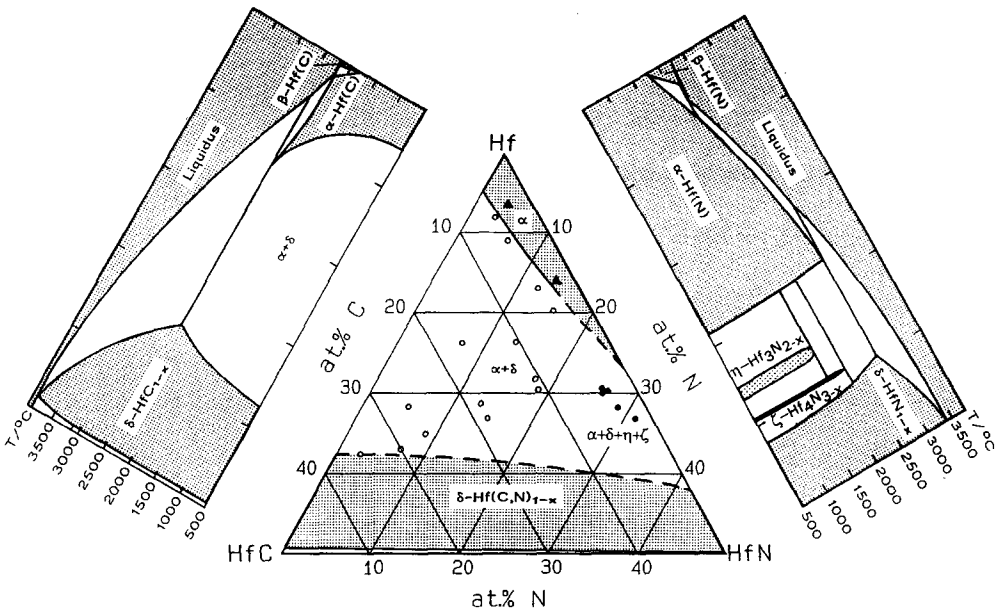

Fig. 4. Results for the Hf–C–N system at 1150 °C together with boundary systems [4,33]; the phase reactions involving the subnitride phases could not be unambiguously established: ▲, single-phase samples, α; ○, two-phase samples, $\alpha+\delta$; ●, four-phase samples, $\alpha+\delta+\eta+\zeta$.

compositions using microprobe analysis as well as a clarification of the formation–decomposition kinetics of the ζ-Hf_4N_{3-x} phase will probably make it possible to determine the phase reactions in the subnitride region. Also, a homogenization pretreatment (e.g. 1600 °C) would decrease the diffusion distance to values much below 0.1 mm for the subsequent heat treatment at the equilibration temperature.

Acknowledgments

This work was sponsored by the Jubiläumsfonds der Oesterreichischen Nationalbank under Project 3729. Support through the French–Austrian research cooperation, Project A11, is gratefully acknowledged. Dr. R.G. Kalista, Teledyne Wah Chang AG. (Liechtenstein), kindly supplied the Hf sponge. Mrs. Cathryn Jelinek helped with the preparation of the manuscript.

References

[1] E.K. Storms, *The Refractory Carbides*, Academic, New York, 1968.
[2] P. Ettmayer and W. Lengauer, Carbides: transition metal solid state chemistry, in *Encyclopedia of Inorganic Chemistry*, Wiley, New York, 1994, in press.
[3] C.H. de Novion, B. Beuneu, T. Priem, N. Lorenzelli and A. Finel, in R. Freer (ed.), *The Physics and Chemistry of Carbides, Nitrides and Borides*, Kluwer, Dordrecht, 1990, p. 329.
[4] T.B. Massalski (ed.), *Binary Alloys Phase Diagrams*, ASM International, Metals Park OH, 1991.
[5] P. Ettmayer and W. Lengauer, Nitrides: transition metal solid state chemistry, in *Encyclopedia of Inorganic Chemistry*, Wiley, New York, 1994, in press.
[6] H. Okamoto, *Bull. Alloy Phase Diag., 11* (1990) 146.
[7] W. Lengauer, *Acta Metall. Mater., 39* (1991) 2985.
[8] W. Lengauer, D. Rafaja, R. Täubler, C. Kral and P. Ettmayer, *Acta Metall. Mater., 41* (1993) 3505.
[9] C. Agte and K. Moers, *Z. Anorg. Allg. Chem., 198* (1931) 233.
[10] R. Kieffer, H. Nowotny, P. Ettmayer and G. Dufek, *Metall (Berlin), 26–27* (1972) 701.
[11] W. Lengauer, S. Binder, K. Aigner, P. Ettmayer, A. Guillou, J. Debuigne and G. Groboth, *J. Alloys Comp., 217* (1995) 137.
[12] P. Duwez and F. Odell, *J. Electrochem. Soc., 97* (1950) 299.
[13] G.M. Klimashin, L.V. Kozlovskii and A.K. Tszyu, *Zh. Prikl. Khim., 44*(7) (1971) 1644.
[14] P. Grieveson, *Proc. Br. Ceram. Soc., 8* (1967) 137.
[15] B.F. Mitrofanov, Y.G. Zainulin, S.I. Alyamovskii and G.P. Shveikin, *Izv. Akad. Nauk SSSR, Neorg. Mater., 10* (1974) 745.
[16] M.P. Arbuzov, S.Y. Golub and B.V. Khaenko, *Inorg. Mater., 14* (1978) 1126.
[17] K.I. Portnoi and Y.V. Levinskii, *Zh. Fiz. Khim., 37* (1963) 2627.
[18] K.I. Portnoi and Y.V. Levinksii, *Issled. Splavov Tsvetn. Metall., Akad. Nauk SSSR, Inst. Met., 4* (1963) 279.
[19] R. Kieffer, H. Nowotny, P. Ettmayer and M. Freudhofmeier, *Monatsh. Chem., 101* (1970) 65.
[20] H. Pastor, *Mater. Sci. Eng. A, 105–106* (1988) 401.
[21] L. Stone and H. Margolin, *Trans. AIME*, (1953) 1498.
[22] F. Teyssandier, M. Ducarroir and C. Bernard, *Calphad, 8* (1984) 233.
[23] S. Jonsson, *Thesis*, Division of Physical Metallurgy, Royal Institute of Technology, Stockholm, 1993.
[24] H. Bittner, H. Goretzki, F. Benesovsky and H. Nowotny, *Monatsh. Chem., 94* (1963) 518.

[25] K. Constant, R. Kieffer and P. Ettmayer, *Monatsh. Chem., 106* (1975) 823.
[26] I.N. Danisina, Y.N. Vil'k, R.G. Avarbe, Y.A. Omel'chenko and T.P. Ryzhkova, *Zh. Prikl. Khim., 41*(3) (1968) 492.
[27] H. Nowotny, F. Benesovsky and E. Rudy, *Monatsh. Chem., 91* (1960) 348.
[28] K. Constant, R. Kieffer and P. Ettmayer, *Monatsh. Chem., 106* (1975) 973.
[29] G. Brundiers, *Nuclear Research Centre Karlsruhe, Rep. KfK-Ext. 6/74-2*, 1974, p. 47.
[30] R. Täubler, S. Binder, M. Groschner, W. Lengauer and P. Ettmayer, *Mikrochim. Acta I, 107* (1991) 337.
[31] W. Lengauer, D. Rafaja and P. Ettmayer, *Mater. Sci. Forum*, in press.
[32] M. Billy and B. Teyssedre, *Bull. Soc. Chim. Fr., 5* (1973) 1537.
[33] W. Lengauer, G. Zehetner and P. Ettmayer, in preparation.